



Title: Human blood *PIG-A* mutation and micronucleated reticulocyte flow cytometric assays: Method optimization and evaluation of intra- and inter-subject variation

Authors: Dorothea K. Torous¹, Svetlana L. Avlasevich¹, Mona G. Khattab², Ayesha Baig³, Lawrence J. Saubermann³, Yuhchyan Chen⁴, Jeffrey C. Bemis¹, David P. Lovell⁵, Vernon E. Walker⁶, James T. MacGregor⁷, Stephen D. Dertinger^{1*}

Affiliations:

¹Litron Laboratories, Rochester, New York, USA

²Baylor College of Medicine, Texas Children's Hospital, Dept. Pediatrics, Houston, TX

³University of Rochester Medical Center, Dept. Pediatrics, Rochester, NY

⁴University of Rochester Medical Center, Dept. Radiation Oncology, Rochester, NY

⁵St. George's University of London

⁶University of Vermont, Dept. Pathology and Laboratory Medicine, Burlington, VT

⁷Toxicology Consulting Services, Bonita Springs, FL

*Corresponding author: SDD, Litron Laboratories, 3500 Winton Place, Rochester, NY, 14623; sdertinger@litronlabs.com

Key words: genotoxicity; flow cytometry, chromosomal damage, mutation, biomonitoring

Running Title: Human blood *PIG-A* mutation and micronucleated reticulocyte assays

This article has been accepted for publication and undergone full peer review but has not been through the copyediting, typesetting, pagination and proofreading process which may lead to differences between this version and the Version of Record. Please cite this article as doi: 10.1002/em.22393

Abstract

We previously described flow cytometry-based methods for scoring the incidence of micronucleated reticulocytes (MN-RET) and *PIG-A* mutant phenotype reticulocytes (MUT RET) in rodent and human blood samples. The current report describes important methodological improvements for human blood analyses, including immunomagnetic enrichment of CD71-positive reticulocytes prior to MN-RET scoring, and procedures for storing frozen blood for later *PIG-A* analysis. Technical replicate variability in MN-RET and MUT RET frequencies based on blood specimens from 14 subjects, intra-subject variability based on serial blood draws from 6 subjects, and inter-subject variation based on up to 344 subjects age 0 to 73 years were quantified. Inter-subject variation explained most of the variability observed for both endpoints ($\geq 77\%$), with much lower intra-subject and technical replicate variability. The relatively large degree of inter-subject variation is apparent from mean and standard deviation values for MN-RET ($0.15 \pm 0.10\%$) and MUT RET (4.7 ± 5.0 per million, after omission of two extreme outliers). The influences of age and sex on inter-subject variation were investigated, and neither factor affected MN-RET whereas both influenced MUT RET frequency. The lowest MUT RET values were observed for subjects < 11 years old, and males had moderately higher frequencies than females. These results indicate that MN-RET and MUT RET are automation-compatible biomarkers of genotoxicity that bridge species of toxicological interest to include human populations. These data will be useful for appropriately designing future human studies that include these biomarkers of genotoxicity, and highlight the need for additional work aimed at identifying the sources of inter-individual variability reported herein.

1. Introduction

DNA damage plays integral roles in many human diseases, including cancer, the numerous Mendelian genetic diseases, atherosclerosis, and DNA-repair deficiency diseases [Hoeijmakers, 2009]. In addition to the role genomic damage plays in cancer and other diseases, a consortium of experts at the Health and Environmental Sciences Institute have recently advocated that mutation should be considered an adverse outcome in its own right [Heflich et al., 2020]. Despite its importance, the systematic study of DNA damage and identification of causative factors are hampered by the lack of rapid, sensitive, and economical *in vivo* assays that can be readily applied to human specimens. Adaptation of two flow cytometry-based assays that are widely used for rodent studies to human blood samples may overcome these obstacles—micronucleated reticulocyte (MN-RET) and *PIG-A* mutant reticulocyte (MUT RET) analyses [Dertinger et al., 2004, 2011].

The MN-RET assay is responsive to chromosomal damage that results in DNA double-strand breaks or mal-segregation of chromosomes [Heddle, 1973; MacGregor et al., 1980; Hayashi et al., 2000], and the *PIG-A* assay reports the occurrence of inactivating gene mutations [Araten et al., 1999; Gollapudi et al., 2015]. Together they represent complementary biomarkers that cover a wide range of genotoxic lesions. We anticipate that an efficient and reliable human blood-based strategy for quantifying chromosomal damage and gene mutation would benefit myriad lines of investigation. These include, but are not limited to: identification of genotoxic environmental or occupational exposures; development of pharmaceuticals, consumer products, and industrial chemicals with inherently lower genotoxicity; identification of unhealthy lifestyle choices; studying the consequences of diagnostic and therapeutic radiation; identifying subjects at high risk for certain diseases; and detection of genotypes associated with increased rates of DNA damage.

This laboratory and others have previously reported significant progress adapting these rodent assays to human blood analyses [Dertinger et al., 2004, 2007, 2015; Grawé et al., 2005;

Offer et al., 2005; Witt et al., 2007; Dobrovolsky et al., 2011; Horibata et al., 2016; Cao et al., 2016, 2020a,b; Khattab et al., 2017; Haboubi et al., 2019]. Here, we report methodological improvements that overcome barriers to wide-spread use. One obstacle stems from the fact that the flow cytometric approach to scoring peripheral blood micronuclei is based on the analysis of the most immature fraction of erythrocytes, i.e., the CD71-positive fraction of reticulocytes, which are present at a very low frequency of about 0.1% in the human blood circulation. Focusing analyses on these most immature reticulocytes is advantageous because it minimizes the impact of splenic filtration function has on micronucleated erythrocyte frequencies [Dertinger et al., 2004, 2007]. However, this low frequency has made it challenging to interrogate adequate numbers of reticulocytes to precisely measure %MN-RET. Informed by work by Grawé and colleagues [2005], we have developed an immunomagnetic method that overcomes this problem by enriching CD71-positive reticulocytes prior to flow cytometric analysis.

Another limitation has been the requirement to label and analyze blood samples for the *PIG-A* assay within several days of collection. Here, we report that methods recently developed for freezing and later thawing rodent blood samples for mutation analysis [Avlasevich et al., 2019] are effective with human blood. This is an important advance that overcomes numerous logistical issues that would otherwise interfere with many, if not most, human biomonitoring studies.

Another significant barrier to routinely incorporating MN-RET and MUT RET biomarkers into human population studies has been the scarcity of data from presumably healthy human subjects. In order to design adequately powered studies, it is important to understand the distribution of healthy volunteer data once technical sources of variability have been minimized, and to be cognizant of host factors that have an appreciable influence on MN-RET and MUT RET frequencies. Therefore, after optimizing these assays, we assessed technical replicate variability and intra-subject variability over a 5-week period based on ≥ 6 individuals, and inter-subject variation based on ≥ 344 individuals. We also investigated the influence of age and sex

on MN-RET and MUT RET frequencies. The results of these experiments form the basis of the recommendations we provide for effectively incorporating these biomarkers into human biomonitoring studies.

2. Materials and Methods

2.1 Mouse Study

2.1.1 Mice

Male CD-1 mice were purchased from Jackson Laboratories (Bar Harbor, Maine). Mice were allowed to acclimate for at least one week prior to treatment, and were handled in accordance with the standards established by the U.S. Animal Welfare Acts set forth in the National Institutes of Health (NIH) guidelines. All procedures were reviewed and approved by the University of Rochester's Committee on Animal Resources. Purina Mills Rodent Chow 5001 and water were available *ad libitum*.

2.1.2 Mouse Blood Micronucleus Assay: Reagents

Absolute methanol and heat-inactivated fetal bovine serum (FBS; cat. no. 89510-186) were from VWR, Radnor, PA. Reagents used for flow cytometric MN-RET scoring (Anticoagulant Solution, Buffer Solution, DNA Stain, Anti-CD71-FITC and Anti-CD61-PE Antibodies, RNase Solution, and Malaria Biostandards) were from *In Vivo* MicroFlow® PLUS-M Kits, Litron Laboratories, Rochester, NY. FITC Selection Cocktail and Magnetic Nanoparticles (cat. no. 18555) were from STEMCELL Technologies Inc., Vancouver, Canada.

2.1.3 Treatment, Blood Collection

At the time of treatment mice were approximately 6 weeks old. Ionizing radiation doses were 0.5, 1, 2, and 4 Gy, and sham irradiation was used as the negative control. Three mice were randomly selected for each group, and total body irradiation was performed with a single

exposure to ^{137}Cs gamma rays. The dose rate was approximately 2 Gy per minute. After irradiation, the mice were maintained in groups of 3 per cage in a pathogen-free room. Blood samples were collected 24 hr post-exposure *via* an incision to a tail vein after mice were warmed briefly under a heat lamp. Approximately 50 μL of free-flowing blood was collected into tubes containing 200 μL kit-supplied Anticoagulant Solution which was maintained at room temperature until fixation occurred (within 4 hr). Blood samples were fixed with ultracold methanol according to Mouse MicroFlow^{PLUS} Kit instructions. These fixed blood specimens were returned to the ultracold freezer for storage until flow cytometric analyses were performed as described below.

2.1.4 Mouse Blood Micronucleus Assay: Sample Processing and Flow Cytometric Analysis

Fixed blood samples were washed out of methanol, cells were pelleted *via* centrifugation, and supernatants were aspirated according to manufacturer recommendations (*In Vivo* MicroFlow[®] PLUS-M Kit instruction manual, www.litronlabs.com). Tubes were gently tapped to resuspend the cells and 100 μL of Buffer Solution were added. The entire volume of each tube was transferred into a new 96-well round bottom assay plate (Falcon cat. no. 353910) with pre-aliquoted 100 μL working Labeling Solution (anti-CD71-FITC, anti-CD61-PE and RNase). Samples were incubated for 30 min at 4°C and then 30 min at room temperature, at which point cells were resuspended by gentle pipetting and transferred directly into 1.5 mL ice-cold Buffer + 1% FBS that was pre-aliquoted into wells of a 96-well deep-well plate (Axygen Scientific cat. no. P-DW-20-C). Cells were collected *via* centrifugation at 340 x g for 5 min. After centrifugation and aspiration of supernatant, cells were resuspended in 75 μL ice-cold Buffer Solution and kept cold and protected from light. A small aliquot (10 μL) of each cell suspension was transferred to a 96-well round bottom plate containing 50 μL of ice-cold Buffer and was

used for standard MicroFlow sample analysis and stored at 4°C until flow cytometric analysis occurred as described below (same day).

The remainder (majority) of each sample was used for reticulocyte enrichment. The entire volume of labeled cells was moved to a new well of a 96-well round bottom assay plate (Falcon cat. no. 353910) containing 50 μ L of FITC selection cocktail (5 μ L per 100 μ L of Buffer), mixed gently by pipetting, and incubated at room temperature for 15 min. Cells were then moved to a new set of wells containing 50 μ L of magnetic nanoparticles, mixed well and incubated for 10 min at room temperature. Cell suspensions (150 μ L) were transferred to a new set of wells on a standard 96-well round bottom plate and a 96-well format Magnetic Bead Extractor (V&P Scientific's Magnetic Bead Separation Extractor, cat. no. 407AM-N) that was sheathed with a PCR cover plate (V&P Scientific's PCR plate, cat. no. VP 407AM-N-PCR). The magnetic beads with attached CD71-FITC cells were extracted from the cell mixture after 10 min incubation at room temperature. The magnet and cover were then moved into wells of a sister plate containing 150 μ L per well pre-aliquoted DNA Staining Solution. At this point, the cover plate was detached from the magnetic pins and the beads were released into the DNA Staining Solution. The plate was stored at 4°C and protected from light until flow cytometric analysis occurred as described below (same day).

Samples were analyzed by a flow cytometer equipped with a 488-nm laser (FACSCanto™ II running FACSDiva™ v6.1.3, Becton Dickinson, San Jose, CA). Anti-CD71-FITC, anti-CD61-PE, and propidium iodide fluorescence signals were detected in the FITC, PE, and PerCP-Cy5.5 channels, respectively. The gating logic used to ensure that quantitative analyses of erythrocyte subpopulations were not contaminated by other cellular or noncellular events has been described previously [Dertinger et al., 2004]. Calibration of the flow cytometer was accomplished by staining malaria-infected erythrocytes in parallel with test samples on each day of analysis [Tometsko et al., 1993]. The stop mode was set so that 20,000 CD71+

RETs per blood sample were evaluated for micronuclei, and the percentage of MN-RET and RET were calculated with Microsoft® Excel for Mac (v16.16.14).

2.1.5 Statistical Analyses

Each mouse blood sample was split between two methods to generate %MN-RET values—standard MicroFlow analysis, and MicroFlow analysis following immunomagnetic enrichment of CD71+ RET. A linear fit was calculated in Excel. The resulting slope factor (m) was used to characterize accuracy, while the correlation coefficient (r^2) was calculated to describe precision. As described in the fundamental works of Altman and Bland [1983], a correlation analysis does not describe measurement performance sufficiently. Therefore, the methodology proposed by Bland and Altman was also applied, also using Excel. In doing so, differences versus averages of %MN-RET values with and without immunomagnetic separation were plotted to describe bias and dispersion structures. Upper and lower limits of agreement were calculated to provide additional quantitative information about method performance.

2.2 Human Subject Studies

2.2.1 Subject Information

363 subjects, all under IRB-approved protocols, provided informed consent and donated blood sample(s) *via* venipuncture of the median cubital or cephalic vein at the cubital fossa. Blood was collected into a single 4 or 10 mL K₂-EDTA vacutainer tube. The sources of the blood samples and subject characteristics are described in Table I. Thirty-seven volunteers provided blood samples at the University of Rochester Medical Center or an affiliated clinic, in which case the local samples were transported to Litron in Exakt Paks with -20°C ice packs to keep them cold but not frozen during same day delivery. The majority of the samples (300) were purchased from Biological Specialty Company (Colmar, PA). These samples, as well blood collected at Texas Children's Hospital, required overnight transportation. In these cases, K₂-EDTA vials

were shipped in Exakt Pak or comparable containers with -20°C ice packs in order to keep them cold, not frozen during FedEx First Overnight delivery service.

2.2.2 Human Blood Micronucleus Assay: Reagents

Absolute methanol and heat-inactivated fetal bovine serum (FBS; cat. no. 89510-186) were from VWR, Radnor, PA. Reagents used for flow cytometric MN-RET scoring (Anticoagulant Solution, Buffer Solution, DNA Stain, Anti-CD71-FITC and Anti-CD61-PE Antibodies, RNase Solution, and Malaria Biostandards) were from Prototype *In Vivo* MicroFlow® PLUS-H Kits, Litron Laboratories, Rochester, NY. Anti-FITC MicroBeads, MS Columns, and an OctoMACS™ Separator were from Miltenyi Biotec, Bergisch Gladbach, Germany.

2.2.3 Human Blood Micronucleus Assay: Sample Processing and Flow Cytometric Analysis

The methods for preparing human blood samples for MN-RET scoring are similar to those described previously [Dertinger et al., 2004, 2007]. However, after incubating fixed blood samples with RNase, anti-CD71-FITC, and anti-CD61-PE, the cells were exposed to an anti-FITC microbead solution. That is, superparamagnetic anti-FITC MicroBeads in Buffer Solution + 1% FBS (5 µL /100mL) were added to each sample in a volume of 100 µL and were mixed with gentle pipetting. Following a 30 min incubation at 4°C, 1 mL cold Buffer Solution + 1% FBS was added to each sample and cells were mixed with gently pipetting. Each sample was divided into two fractions: “pre-column” and “post-column”. For pre-column samples, a 20 µL aliquot of each cell suspension was added to 280 µL working DNA Stain and samples were placed on ice or at 4°C until flow cytometric analysis occurred as described below (same day). The remainder (majority) of each sample was applied to a pre-wetted Miltenyi MS Column suspended in an OctoMACS Separator. Once all of the unlabeled cells passed through the column, each MS

column was washed three times with 500 μ L Hank's Balanced Salt Solution + 1% FBS. At this point each MS column was removed from the magnetic field and placed onto a 15 mL centrifuge tube. Two mL Hank's Balanced Salt Solution + 1% FBS was added to each column reservoir to gently flush out the bound reticulocytes using the plunger supplied with the columns. After centrifugation (5 min at 800 x g) and aspiration, cell pellets were tapped loose, and stored on wet ice until flow cytometric analysis occurred as described below (same day).

At the beginning of each FCM analysis day, instrumentation and acquisition/analysis software parameters were calibrated based on the fluorescence of a biological standard— kit supplied malaria-infected rat blood (methanol fixed). As described previously, this sample guided photomultiplier tube voltages and compensation settings to resolve parasitized reticulocytes and also guided the position of the micronucleus scoring region. Data acquisition and analyses were performed using a FACSCalibur flow cytometer providing 488 nm excitation, running CellQuest™ Pro software v5.2.

Once photomultiplier tube voltages and compensation settings were configured with the malaria biostandard, the pre- and post-column paired samples were analyzed. Pre-column sample data acquisition occurred until 300,000 total erythrocytes were collected. While the pre-column sample was being analyzed, 300 μ L of the same working DNA stain was added to each post-column tube and the entire volume was transferred into a standard flow cytometer tube. Each sample was analyzed so that at least 10,000, but preferably 20,000 CD71-positive RET were analyzed. Note that we do not report %MN-RET for 18 of 356 samples (5% of total) because pre-column RET was < 0.02% and we were unable to acquire at least 10,000 RET.

2.2.4 Human Blood PIG-A Assay: Reagents

Lympholyte®-H was purchased from CedarLane, Burlington, NC. Anti-PE MicroBeads, LS Columns, and QuadroMACS™ Separator were from Miltenyi Biotec, Bergisch Gladbach, Germany. CountBright™ Absolute Counting Beads and fetal bovine serum (FBS) were

purchased from Invitrogen, Carlsbad, CA. Anticoagulant Solution, balanced salt solution (BSS), Nucleic Acid Dye Solution (a 1000-fold dilution of SYTO® 13 dye in DMSO), anti-human-CD59-PE (clone OV9A2), anti-human-CD55-PE (clone 143–30), anti-human-CD45-PE (clone HI30), and anti-human-CD61-PE (clone VI-PL2) were from Prototype Human MutaFlow® Kits (Litron Laboratories, Rochester, NY). Blood Freezing and Blood Thawing Solutions A and B were from MutaFlow® Blood Freezing and Thawing Kits (Litron Laboratories, Rochester, NY).

2.2.5 Human Blood PIG-A Assay, Sample Processing and Flow Cytometric Analysis

The method for preparing human blood samples for MUT RET scoring is similar to that described previously [Dertinger *et al.*, 2015]. Two differences relative to the initial report are noteworthy. First, we scaled up reagents to label and analyze 200 μ L blood (or 240 μ L of frozen/thawed blood) per specimen as opposed to 100 μ L. Second, since an effective blood freezing and thawing protocol was established (described below), a large portion of the *PIG-A* data reported herein were from samples that were frozen and later thawed for deferred flow cytometric analysis.

Freezing Solution (1 mL) was aliquoted into pre-labeled cryovials prior to freezing and maintained at room temperature. Upon receipt, human whole blood cells were gently resuspended by pipetting and 240 μ L of blood was transferred into the Freezing Solution. Samples were incubated in Freezing Solution at room temperature for 5 min then transferred to a -75 to -85°C freezer. Samples were frozen for at least 48 hr before *PIG-A* analysis.

On the day of FCM analysis, up to 12 frozen blood samples were removed from the ultracold freezer and quickly thawed in a 37°C water bath. Once thawed (about 2 min), blood suspensions were moved to new pre-labeled 50 mL centrifuge tube. 0.9 mL Thawing Solution A was added to each tube and mixed by gentle pipetting up and down 6-8 times. Blood samples were incubated at room temperature for 5 min. After incubation, 4.5 mL Thawing Solution B was added to each tube and mixed by gentle pipetting followed by 5 min incubation at room

temperature. Thawing Solution B was added again at 5 min intervals, first 5.4 mL and then 28.8 mL. After the final 5 min incubation, samples were centrifuged at 340 x g for 5 min, supernatants were aspirated, 100 μ L BSS were added to each tube, and the cells were resuspended with gentle pipetting.

The entire volume of each thawed blood sample was layered onto 1.5 mL room temperature Lympholyte-H that was pre-aliquoted into wells of a deep-well 96-well plate (Axygen Scientific, 2 mL deep-well plate, cat. no. P-DW-20-C). In the case of never-frozen blood, 200 μ L of blood was layered onto the Lympholyte-H. The plate was centrifuged at 800 x g for 20 minutes and supernatants were aspirated with a multi-channel aspirator with a fixed bridge (V&P Scientific, San Diego, CA). The platelet/leukocyte-depleted pellets were resuspended by gentle pipetting after 130 μ L BSS were added to each well. The contents of each well were washed with an additional 1.5 mL cold BSS + 2%FBS that was pre-aliquoted into a new 96-well deep-well plate and the cells were collected *via* centrifugation for 10 min at 235 x g. 100 μ L BSS were added to each well and the erythrocyte-enriched pellets were mixed by gentle pipetting, and 190 μ L of each were transferred to new wells of the deep-well plate containing 200 μ L working antibody solution (300 μ L anti-CD59-PE stock, 12.5 μ L anti-CD55-PE, 100 μ L anti-CD61-PE, 50 μ L anti-CD45-PE in 537.5 μ L BSS + 2% FBS). After cells were incubated with antibodies for 30 min at 4°C, cells were resuspended with gentle pipetting using a multi-channel pipettor and then transferred to new wells of a deep-well plate with pre-aliquoted 1.5 ml of BSS + 2% FBS. Following centrifugation for 5 min at 340 x g, the supernatants were aspirated using a multi-channel bridge aspirator and 200 μ L superparamagnetic anti-PE MicroBeads in BSS + 2% FBS (300 μ L per mL) were added to each well. Cells and beads were mixed and incubated at 4°C for 30 min, 1.5 mL BSS + 2% FBS were added to each well after incubation and cells were mixed by gentle pipetting. The plate was centrifuged at 340 x g for 5 min, and supernatants were removed with a multi-channel fixed bridge aspirator, then 1 mL BSS + 2% FBS was added to each well and mixed by gentle pipetting. To prepare a pre-column

sample, 10 μ L of each sample were added to 990 μ L BSS with Nucleic Acid Dye Solution and CountBright Absolute Counting Beads (30 μ L/mL). The pre-column samples were incubated at room temperature and protected from light for 30 min, after which time they were stored on ice until flow cytometric analysis occurred as described below. The remainder of each sample was applied to a pre-wetted Miltenyi LS Column suspended in a QuadroMACS Separator. Once the column reservoir was empty, 5 mL BSS + 2% FBS were added to ensure mutant phenotype cells were fully eluted (and collected into a 15 mL polypropylene tube). The eluates were centrifuged for 5 min at 800 x g, supernatants were aspirated, the pellets were tapped loose, and 300 μ L of the same preparation of BSS with Nucleic Acid Dye Solution and CountBright Beads used to prepare pre-column samples were added to each pellet. These post-column samples were incubated at room temperature and protected from light for 30 min. Samples were then placed on ice until flow cytometric analysis occurred as described previously on the same day [Dertinger et al., 2015].

Samples were analyzed by a flow cytometer equipped with a 488-nm laser (FACSCalibur, BD, San Jose, CA). Nucleic Acid Dye, anti-CD59-PE, anti-CD55-PE, anti-CD45-PE, anti-CD61-PE, and Counting Beads fluorescence signals were detected in the FITC, PE, and PerCP-Cy5.5 channels. Calibration of the flow cytometer was accomplished by generating an Instrument Calibration Standard on each day data acquisition occurred. The resulting samples provided sufficient numbers of mutant-mimic cells (RBCs that were stained with Nucleic Acid Dye but not incubated with antibody solution), and were used for optimizing photomultiplier tube voltages and fluorescence compensation settings. The position of the mutant mimics also provided a rational approach for defining the vertical demarcation line used to distinguish mutant phenotype cells from wild-type cells.

After PMT voltages and electronic compensation setting were defined with the Instrument Calibration Standard, pre- and post-column samples were moved into standard flow cytometer tubes and analyzed within 2 hours. Data acquisition continued until a specified time: 1

min for every pre-column sample, and 3 min (i.e., until nearly the entire volume was depleted), for each post-column sample.

2.2.6 Statistical Analyses

The formulas used to calculate MUT RET frequencies based on pre- and post-immunomagnetic column data have been published [Dertinger et al., 2012] and are described in MutaFlow kit manuals (www.litronlabs.com). The incidence of MN-RET is expressed as frequency percent, while the incidence of MUT RET is expressed as number per 10^6 cells. For statistical evaluations, MN-RET and MUT RET frequencies were $\log(10)$ transformed.

JMP software's Variability Chart platform was used to study sources of variability in MN-RET and MUT RET frequencies (JMP v12.0.1, SAS Institute Inc., Cary, NC). Specifically, the restricted maximum likelihood (REML) estimation of variance components was utilized, with the specification "nested" model type. REML is a statistical method that is a modification of maximum likelihood estimation, which allows the generalization of the 'classic' regression and analysis of variance (ANOVA) statistical techniques to a wider series of experiments. For more information, the interested reader is directed to Corbeil and Searle, 1976. We utilized REML to evaluate the variability of MUT RET values attributable to subject, blood storage condition, and technical replicate. In other instances, REML was used to evaluate variability of MN-RET and MUT RET values attributable subject, blood collection time, and technical replicate.

Two-way ANOVA was used to investigate whether the factors age group, sex, and age group x sex interaction significantly affected MN-RET and MUT RET frequencies (JMP v12.0.1). Significance was evaluated at the 5% level. For these analyses, each subject was categorized into one of eight age groups: <1, 1-10, 11-20, 21-30, 31-40, 41-50, 51-60, and 61+ years of age. When two-way ANOVA was significant, a Tukey-Kramer test was used to identify the source of the variation ($\alpha = 0.05$).

JMP software's fit Y by X platform was used to plot MN-RET and MUT RET frequencies

against subject age. Linear and polynomial curves were fitted, and the reported p -values represent a test of the hypothesis that the true slope coefficients are zero. Said another way, the test evaluates whether a particular fitted model explains the data significantly better than a mean fit line. Note that, in the case of MUT RET, these analyses were broken out by sex, since two-way ANOVA had indicated these values were affected by sex. A similar fit Y by X analysis was performed to consider the relationship between individuals' MN-RET and MUT RET frequencies.

Regression analysis was performed for every subjects' MUT RET and corresponding mutant erythrocyte (mutant RBC) frequencies. Additionally, Bland-Altman analysis was performed based on differences versus averages of MUT RET and mutant RBC values in order to describe bias and dispersion structures. Upper and lower limits of agreement were also calculated.

3. Results

3.1. Assay Optimization

3.1.1 Reticulocyte Enrichment for MN-RET Analysis

Proof-of-concept work aimed at enriching RET for the micronucleus assay was accomplished with mouse blood. Using gamma-irradiation to generate a range of MN-RET frequencies, we compared flow cytometry-based %MN-RET frequencies that were generated with and without immunomagnetic enrichment of CD71+ RET. Whereas standard processing of blood samples exhibited a mean %RET value of $1 \pm 0.55\%$, those that were enriched for CD71+ cells averaged $67 \pm 29\%$, a 68-fold increase. Even so, Figure 1 shows MN-RET frequencies for samples split between the standard flow cytometric analysis and those enriched for CD71+ RET exhibited very similar values. Indices of assay precision and accuracy were high, with r^2 and m

values of 0.97 and 0.96, respectively. Bland-Altman analysis revealed little bias (0.09% MN-RET), with relatively narrow upper and lower levels of agreement.

Success with mouse blood encouraged us to develop an analogous RET-enrichment method for the human blood micronucleus assay. The most satisfactory results were obtained with the MACS[®] cell separation platform. Whereas the majority of human blood samples exhibited CD71+ RET frequencies in the range 0.1 to 0.3% prior to separation, post-immunomagnetic column samples averaged 26%—on the order of 100-times more concentrated. Figure 2 shows %MN-RET data from column-enriched samples for 14 different volunteers (5 males, 9 females). Each blood sample was split into 3-4 technical replicates. Since several volunteers provided multiple blood samples over a 5-week period, it was possible to evaluate inter- as well as intra-subject MN-RET variation. Based on REML analysis, the vast majority of variability is attributable to inter-subject differences (77.3%), with much less variability due to technical replicate (17.3%) or intra-subject variation (5.4%). (Note that for Figure 2 and others that display log transformed data, the visual impact of the between individual variability is reduced.)

3.1.2 Blood Storage for PIG-A Analysis

The blood freezing and thawing method that has been proven effective for rodent samples was evaluated for its compatibility with human blood-based *PIG-A* analyses. Results for eight subjects are provided in Figure 3, and shows mutation frequency data under three blood storage conditions: i) analyzed within 24 hr, ii) refrigerated for up to 5 days, and iii) frozen/thawed. REML analysis indicated that technical replicates and storage condition contributed low levels of variability to MUT RET frequencies—18.5 and 0%, respectively. The majority of the observed variability (81.5%) was attributable to inter-subject differences.

Figure 4 shows MUT RET data from the same 14 volunteers that were analyzed for %MN-RET (i.e., Figure 2). Each blood sample was divided into 3-4 technical replicates before

storage and subsequent processing for MUT RET frequency determinations. Since several volunteers provided multiple blood samples over a 5-week period, it was possible to evaluate inter- as well as intra-subject MUT RET variation. Based on REML analysis, the vast majority of variability is attributable to inter-subject differences (90.9%). Again, considerably less variability was explained by technical replicate (9.1%) or intra-subject variation (0%).

3.2 Investigating Sources of Inter-Subject Variation

3.2.1 MN-RET: Age and Sex Effects

Using the optimized MN-RET assay, we investigated the effects of age and sex. Figure 5 shows MN-RET frequencies for 338 individuals as a function of age, with sexes indicated by different symbols. The values ranged from 0.01 to 0.79%, and the overall mean and standard deviation was $0.146 \pm 0.10\%$.

Visually, no age- or sex-effect is apparent. This qualitative impression is supported by several analyses. First, means and standard deviations for %MN-RET are very similar for males and females— $0.15 \pm 0.10\%$ and $0.14 \pm 0.10\%$, respectively. Second, when subjects are categorized by age (< 1, 1-10, 11-20, 21-30 yr, etc.), two-way ANOVA results indicate that neither age group, sex, or an age group x sex interaction effect reaches statistical significance ($p = 0.14, 0.34, \text{ and } 0.53$, respectively). Finally, when age is treated as a continuous variable, the mean fit line is found to describe the data as well as a best fit line ($p = 0.49$).

3.2.2 MUT RET: Age and Sex Effects

Using the optimized PIG-A assay, we investigated the effects of age and sex on MUT RET frequency. Figure 6 shows MUT RET frequencies for 344 individuals as a function of age, with sexes indicated by different symbols. The values ranged from 0 to $1109 \text{ MUT RET} \times 10^{-6}$, and the overall mean and standard deviation was $8.9 \pm 62 \times 10^{-6}$. When two extreme outliers are excluded, the values ranged from 0 to $40.7 \text{ MUT RET} \times 10^{-6}$, and the overall mean and standard

deviation was $4.7 \pm 5.0 \times 10^{-6}$.

Visually, Figure 6 (left panel) suggests age and sex may influence MUT RET frequencies. These qualitative impressions are supported by several quantitative analyses. First, excluding two extreme (high) outliers, the mean MUT RET frequency is modestly elevated in males— 5.9 ± 6.2 compared to 3.5 ± 3.3 per million for females. Second, when subjects are categorized by age group (< 1, 10-11, 11-20, 21-30 yr, etc.), two-way ANOVA results indicate that age group and sex reach statistical significance ($p < 0.001$ for both; whereas age group x sex interaction $p = 0.01$). Finally, when age is treated as a continuous variable, polynomial (cubic) fits describe the data significantly better than mean fit lines ($p < 0.001$ in the case of females and males; see Figure 6 middle and right panels).

Having identified age as a significant factor, we used the decade of age categorization to evaluate responsible group(s). A graphical representation of pair-wise test results is shown in Figures 7 and 8—females and males, respectively. The age group < 1 yr was found to exhibit significantly lower MUT RET values than every other age group except for 1-10 (low N), and this was evident irrespective of sex. In the case of males, one other significant difference was evident between the age groups 21-30 and 51-60, with higher values observed with increased age. Note that while males 61+ actually exhibited the highest mean MUT RET value, the number of subjects in this group was low compared to each of the other groups.

3.3 Relationship Between Biomarkers

Figure 9 shows each subjects' MN-RET value graphed against their corresponding MUT RET value. There is a striking lack of correlation between these two biomarkers. Indeed, the meant fit line explains the relationship between the two biomarkers as well as a best fit line ($p = 0.82$).

PIG-A assay results have focused on the youngest fraction of circulating erythrocytes, the RET cohort. This decision is based on the fact that in the case of human blood circulation,

mutant phenotype erythrocytes exhibit a shortened lifespan [Ware et al., 1995]. Data generated over the course of the current experiments supports this view. Figure 10 (left panel) shows each subject's MUT RET frequency graphed against the corresponding mutant RBC frequency. While the values are clearly correlated, the resulting slope (1.23) indicates that mutant RBC are considerably lower than MUT RET. This is reinforced by the Bland-Altman analysis (Figure 10, right panel). Beyond showing a negative bias, the dispersion structure indicates the bias is not uniform. Rather, as MUT RET values increase, the more mutant RBC values underestimate them.

4. Discussion

4.1 Major Findings

The results presented herein support the effectiveness and reliability of the new processing methods that include enrichment of CD71+ RET for subsequent MN-RET scoring, and storage of blood samples for deferred *PIG-A* assay analysis. These updated methods overcome technical issues that would have otherwise represented challenging obstacles to many, if not most, human biomonitoring applications.

Using the improved methodology, we found the variability of MN-RET and MUT RET measurements to be dominated by inter-subject variation, with only a minor contribution from intra-subject variability—at least over a 5-week period. Our analysis of hundreds of relatively healthy individuals over a wide range of ages suggest that neither age or sex significantly influence MN-RET frequency over the age range studied, 0 - 73 yr. On the other hand, MUT RET values were affected by age and sex, with the lowest frequencies being observed in the youngest subjects, and with males exhibiting moderately higher frequencies than females. It is important to acknowledge that, while these factors attained high statistical significance, some of the absolute differences were relatively modest. For instance, the overall mean MUT RET frequency for females and males was 3.5×10^{-6} versus 5.9×10^{-6} , respectively. The age effect

appeared to be more substantial. For instance, in the case of the age groups < 1 and 60+ yr, males exhibited mean MUT RET frequencies of $0.6 \pm 0.5 \times 10^{-6}$ versus $10.4 \pm 2.9 \times 10^{-6}$, respectively.

4.2 Recommendations

The results presented herein have important implications for designing human biomonitoring studies using these genotoxicity biomarkers.

- i. Given the effect that age and sex have on MUT RET frequencies, it will be important to balance experimental groups with these factors in mind. This design element would appear to be less critical in the case of the MN-RET endpoint.
- ii. We found that for both the MN-RET and MUT RET biomarkers, the majority of the variability is attributable to inter-subject differences, with little effect of blood collection time (i.e., intra-subject variability). Consequently, relatively large numbers of volunteers will be necessary to adequately power human biomonitoring studies when comparisons are restricted to differences among subjects. On the other hand, lower numbers of volunteers will be necessary for experimental designs that are compatible with the collection of pre-intervention blood samples. In these cases, subject-specific baseline MN-RET and/or *PIG-A* mutation values will be available for consideration, an experimental design that will significantly reduce the number of study participants necessary to achieve a given level of statistical power.
- iii. There was a marked absence of correlation between individuals' MN-RET and MUT RET frequencies. For several reasons, this was an anticipated result. First, these biomarkers reflect distinct types of genomic damage—chromosomal damage versus gene mutation. Second, there are examples of genotoxicant-exposed rodents that have

exhibited markedly dissimilar MN-RET and MUT RET responses [Dertinger et al., 2012; Bhalli et al., 2013; Guérard et al., 2013; Elhajouji et al., 2018]. Third, MacGregor and colleagues [1997] reported a similar lack of correlation among several diverse human blood genotoxicity endpoints. With this information, investigators that are interested in adding a genotoxicity component to their human biomonitoring studies are advised to conduct multiple, complementary assays. The cost of performing multiple assays is incremental and modest compared to the costs associated with subject recruitment and other considerations, and the value added has the potential of being dramatic. This added value is readily accomplished by combining the MN-RET and *PIG-A* assays given their low blood volume requirements and the complementary nature of the genomic damage detected.

- iv. MUT RET and MUT RBC frequencies are correlated, and as expected, MUT RBC values consistently underestimate MUT RET frequencies. While systematic underestimation may not always be problematic, we are more concerned that Bland-Altman analysis shows a skewed dispersion structure whereby MUT RBC more greatly underestimate MUT RET as mutant cell frequencies increase. It is a fact that MUT RET analysis requires more resources relative to MUT RBC analysis—the former requires immunomagnetic separation, the latter does not. Even so, the MUT RET endpoint is demonstrably the preferred population of erythrocytes to study in the case of human blood biomonitoring studies.

4.2 Future Studies

Even in the case of MUT RET, where age and sex were found to be significant factors, the majority of the variability remains unexplained. Future work is needed to identify host and environmental factors that are responsible for inter-subject differences in MN-RET and MUT

RET frequencies. That information would contribute to the design of more efficient human blood genotoxicity biomonitoring studies and would add fundamental knowledge to the field of cancer research, which considers genomic damage a key factor in the multistep process of carcinogenesis [Hanahan and Weinberg, 2000, 2011].

AUTHOR CONTRIBUTIONS

M.G.K., A.B., L.J.S., Y.C., J.C.B., and V.E.W. gained the approvals necessary to conduct human subject research at their respective institutions. J.C.B., D.P.L., J.T.M., and S.D.D. designed the scale and scope of the study. M.G.K., A.B., and Y.C. oversaw recruitment of volunteers, and D.K.T. managed the purchasing and scheduling of commercially-supplied blood samples. D.K.T. and S.L.A. performed the blood processing and flow cytometric analyses. Statistical analyses were performed by S.D.D. under the guidance of D.P.L. S.D.D. wrote a draft manuscript, and all authors contributed to the substantial revisions that followed.

ACKNOWLEDGMENTS

This work was funded by a grant from the National Institute of Health/National Institute of Environmental Health Sciences (NIEHS; grant number R44ES028163). The contents are solely the responsibility of the authors, and do not necessarily represent the official views of the NIEHS. The authors would like to thank the important contributions to this work by Ying Tsai (mouse irradiation), Therese Smudzin and Cathy Zimmermann (IRB approval and recruitment of volunteers), and Merrie Lou Nagel (phlebotomy).

CONFLICT OF INTEREST STATEMENT

D.K.T., S.L.A., J.C.B and S.D.D are employed by Litron Laboratories. Litron owns patents covering the flow cytometry-based assays described in this manuscript and plans to sell commercial kits based on these procedures: J.T.M. serves as a consultant to Litron.

Figure Legends

Figure 1. Micronucleated reticulocyte (MN-RET) frequencies are graphed for mouse blood samples that were each processed in two manners: immunomagnetically enriched versus not enriched for CD71-positive reticulocytes prior to flow cytometric analysis. The left panel shows linear regression and correlation analyses that provide metrics of accuracy ($m = 0.96$) and precision ($r^2 = 0.97$). The right panel shows the difference in MN-RET frequency for each sample in relation to the average value. Bias (solid black line) and upper and lower limits of agreement (dashed lines) were derived from Bland-Altman analysis.

Figure 2. Log₁₀ transformed micronucleated reticulocyte (MN-RET) frequencies are graphed for fourteen volunteers, 5 of which provided blood over a 5-week period. Blood samples were processed as 3-4 technical replicates, and these individual MN-RET measurements are shown. Results from this nested design were evaluated by Restricted Maximum Likelihood analysis and demonstrated that inter-subject, intra-subject (collection time), and technical replicate factors contributed 77.3, 5.4, and 17.3% of the observed variation, respectively.

Figure 3. Log₁₀ transformed mutant reticulocyte (MUT RET) frequencies are graphed for eight volunteers. Each blood sample was processed after being stored under 3 conditions: refrigerated ≤ 24 hr, refrigerated ≤ 5 days, and stored frozen until day of analysis. Blood samples were processed as 4 technical replicates, and these individual MUT RET measurements are graphed. Results from this nested design were evaluated by Restricted Maximum Likelihood analysis and showed that inter-subject, storage condition, and technical replicate factors contributed 81.5, 0, and 18.5% of the observed variation, respectively.

Figure 4. Log₁₀ transformed mutant reticulocyte (MUT RET) frequencies are graphed for

fourteen volunteers, 6 of which provided blood over a 5-week period. Blood samples were processed as 3-4 technical replicates, and these individual mutant measurements are shown. Results from this nested design were evaluated by Restricted Maximum Likelihood analysis and demonstrated that inter-subject, intra-subject (collection time), and technical replicate factors contributed 90.9, 0, and 9.1% of the observed variation, respectively.

Figure 5. Log₁₀ transformed micronucleated reticulocyte (MN-RET) frequencies are graphed versus age (yr), with males as blue squares and females as red triangles. An ANOVA platform indicates that the best linear fit line (green solid line) does not describe the data any better than the mean fit line (orange), $p = 0.49$. The dashed lines correspond to the 95% prediction interval.

Figure 6. Log₁₀ transformed mutant reticulocyte (MUT RET) frequencies are graphed versus age (yr), with males as blue squares and females as red triangles. ANOVA indicates that cubic polynomial fits (orange solid lines) describe the data better than mean fit lines (green lines), $p < 0.001$ for both females (center panel) and males (right panel). The dashed lines correspond to 95% prediction intervals.

Figure 7. Female volunteers' log₁₀ transformed mutant reticulocyte (MUT RET) frequencies are graphed according to age group. Each group mean is indicated by a green line. Circles' diameters represent 95% confidence intervals. Tukey-Kramer test results indicate the age group < 1 yr exhibited significantly lower MUT RET values compared to every other age group except for 1-10 yr (although it should be noted that group has low N).

Figure 8. Male volunteers' log₁₀ transformed mutant reticulocyte (MUT RET) frequencies are graphed according to age group. Each group mean is indicated by a green line. Circles' diameters represent 95% confidence intervals. Tukey-Kramer test results indicate the age group

< 1 yr exhibited significantly lower MUT RET values compared to every other age group except for 1-10 yr (although it should be noted that group has low N). One additional significant difference was identified, between age groups 21-30 and 51-60. Note that while males 61+ actually exhibited the highest mean MUT RET value, the number of subjects in this group was low compared to each of the other groups.

Figure 9. Each subject's log₁₀ transformed micronucleated reticulocyte (MN-RET) frequency is graphed against their corresponding mutant reticulocyte frequency, with males as blue squares and females as red triangles. ANOVA indicates that the best linear fit line (green) does not describe the data any better than the mean fit line (red), $p = 0.82$.

Figure 10. The left panel shows each subjects' mutant reticulocyte (MUT RET) frequency graphed against their corresponding mutant erythrocyte (MUT RBC) frequency. The values are correlated ($r^2 = 0.71$), but show a bias for lower MUT RBC values ($m = 1.23$). The right panel shows the difference in MUT RET and MUT RBC frequency for each sample in relation to the average value. Bias (solid black line) and upper and lower limits of agreement (dashed lines) were derived from Bland-Altman analysis. A linear regression line has been added to highlight the fact that there is a skewed dispersion structure to the data whereby MUT RBC more greatly underestimate MUT RET as mutant cell frequencies increase.

REFERENCES

- Altman, D.G. and Bland, J.M. (1983) Measurement in medicine: The analysis of method comparison studies. *Statistician*, 32, 307-317.
- Araten, D.J., Nafa, K., Pakdeesuwan, K. and Luzzatto, L. (1999) Clonal populations of hematopoietic cells with paroxysmal nocturnal hemoglobinuria genotype and phenotype

are present in normal individuals. *Proceedings of the National Academy of Science USA*, 96, 5209-5214.

Avlasevich, S.L., Torous, D.K., Bemis, J.C., Bhalli, J.A., Tebbe, C.C., Noteboom, J., Thomas, D., Roberts, D.J., Barragato, M., Schneider, B., Pratico, J., Richardson, M., Gollapudi, B.B. and Dertinger, S.D. (2019) Suitability of long-term frozen rat blood samples for the interrogation of *Pig-a* gene mutation by flow cytometry. *Environmental and Molecular Mutagenesis*, 60(1), 47-55.

Bhalli, J.A., Ding, W., Shaddock, J.G., Pearce, M.G., Dobrovolsky, V.N. and Heflich, R.H. (2013) Evaluating the weak in vivo micronucleus response of a genotoxic carcinogen, aristolochic acids. *Mutation Research*, 753(2), 82-92.

Cao, Y., Yang, L., Feng, N., Shi, O., Xi, J., You, X., Yin, C., Yang, H., Horibata, K., Honma, M., Qian, B., Weng, W. and Luan, Y. (2016) A population study using the human erythrocyte *PIG-A* assay. *Environmental and Molecular Mutagenesis*, 57(8), 605-614.

Cao, Y., Wang, X., Liu, W., Feng, N., Xi, J., You, X., Chen, R., Zhang, X., Liu, Z. and Luan, Y. (2020a) The potential application of human *PIG-A* assay on azathioprine treated inflammatory bowel disease patients. *Environmental and Molecular Mutagenesis*, 61, 456-464.

Cao, Y., Wang, T., Xi, J., Zhang, G., Wang, T., Liu, W., You, X., Zhang, X., Xia, Z. and Luan, Y. (2020b) *PIG-A* gene mutation as a genotoxicity biomarker in human population studies: An investigation in lead-exposed workers. *Environmental and Molecular Mutagenesis*, in press, doi: 10.1002/em.22373.

Corbeil, R.R. and Searle, S.R. (1976) Restricted maximum likelihood (REML) estimation of variance components in the mixed model. *Technometrics*, 18, 31-38.

Dertinger, S.D., Camphausen, K., MacGregor, J.T., Bishop, M.E., Torous, D.K., Avlasevich, S., Cairns, S., Tometsko, C.R., Menard, C., Muanza, T. et al. (2004) Three-color labeling

method for flow cytometric measurement of cytogenetic damage in rodent and human blood. *Environmental and Molecular Mutagenesis*, 44, 427-435.

Dertinger, S.D., Miller, R.K., Brewer, K., Smudzin, T., Torous, D.K., Roberts, D.J., Avlasevich, S.L., Bryce, S.M., Sugunan, S. and Chen, Y. (2007) Automated human blood micronucleated reticulocyte measurements for rapid assessment of chromosomal damage. *Mutation Research*, 626, 111-119.

Dertinger, S.D., Bryce, S.M., Phonethepswath, S. and Avlasevich, S.L. (2011) When pigs fly: Immunomagnetic separation facilitates rapid determination of *Pig-a* mutant frequency by flow cytometric analysis. *Mutation Research*, 721, 163-170.

Dertinger, S.D., Phonethepswath, S., Avlasevich, S.L., Torous, D.K., Mereness, J., Bryce, S.M., Bemis, J.C., Bell, S., Weller, P. and MacGregor, J.T. (2012) Efficient monitoring of *in vivo* *Pig-a* gene mutation and chromosomal damage: Summary of 7 published studies and results from 11 new reference compounds. *Toxicological Sciences*, 130, 328-348.

Dertinger, S.D., Avlasevich, S.L., Bemis, J.C., Chen, Y. and MacGregor, J.T. (2015) Human erythrocyte *PIG-A* assay: An easily monitored index of gene mutation requiring low volume blood samples. *Environmental and Molecular Mutagenesis*, 56, 366-377.

Dobrovolsky, V.N., Elespuru, R.K., Bigger, C.A., Robison, T.W. and Heflich, R.H. (2011) Monitoring humans for somatic mutation in the endogenous *PIG-A* gene using red blood cells. *Environmental and Molecular Mutagenesis*, 52(9), 784-794.

Elhajouji, A., Vaskova, D., Downing, R., Dertinger, S.D., Martus, H. (2018) Induction of *in vivo* *Pig-a* gene mutation but not micronuclei by 5-(2-chloroethyl)-2'-deoxyuridine, an antiviral pyrimidine nucleoside analogue. *Mutagenesis*, 33(5-6), 343-350.

Gollapudi, B.B., Lynch, A.M., Heflich, R.H., Dertinger, S.D., Dobrovolsky, V.N., Froetschl, R., Horibata, K., Kenyon, M.O., Kimoto, T., Lovell, D.P. et al. (2015) The *in vivo* *Pig-a* mutation assay: A report of the International Workshop of Genotoxicity Testing (IWGT) Workgroup. *Mutation Research*, 783, 23-35.

- Guérard, M., Koenig, J., Festag, M., Dertinger, S.D., Singer, T., Schmitt, G. and Zeller, A. (2013) Assessment of the genotoxic potential of azidothymidine in the comet, micronucleus, and *Pig-a* assay. *Toxicological Sciences*, 135(2), 309-316.
- Grawé, J., Biko, J., Lorenz, R., Reiners, C., Stopper, H., Vershenya, S. et al. (2005) Evaluation of the reticulocyte micronucleus assay in patients treated with radioiodine for thyroid cancer. *Mutation Research*, 583, 12-25.
- Haboubi, H.N., Lawrence, R.L., Rees, B., Williams, L., Manson, J.M., Al-Mossawi, N., Bodger, O., Griffiths, P., Thornton, C. and Jenkins, G.J. (2019) Developing a blood-based gene mutation assay as a novel biomarker for oesophageal adenocarcinoma. *Scientific Reports*, 9(1), 5168.
- Hanahan, D. and Weinberg, R.A. (2000) The Hallmarks of cancer. *Cell*, 100(1), 57-70.
- Hanahan, D. and Weinberg, R.A. (2011) Hallmarks of cancer: the next generation. *Cell*, 144(5), 646-674.
- Hayashi, M., MacGregor, J.T., Gatehouse, D.G., Adler, I.-D., Blakey, D.H., Dertinger, S.D., Krishna, G., Morita, T., Russo, A. and Sutou, S. (2000) In vivo rodent erythrocyte micronucleus assay: aspects of protocol design including repeated treatments, integration with toxicity testing, and automated scoring—a report from the International Workshop on Genotoxicity Test Procedures (IWGTP). *Environmental and Molecular Mutagenesis*, 35, 234-252.
- Heddle, J. (1973) A rapid in vivo test for chromosome damage. *Mutation Research*, 18, 187-190.
- Heflich, R.H., Johnson, G.E., Zeller, A., Marchetti, F., Douglas, G.R., Witt, K.L., Gollapudi, B.B. and White, P.A. (2020) Mutation as a toxicological endpoint for regulatory decision-making. *Environmental and Molecular Mutagenesis*, 61, 34-41.
- Hoeijmakers, J.H.J. (2009) DNA damage, aging, and cancer. *New England Journal of Medicine*, 361, 1475-1485.

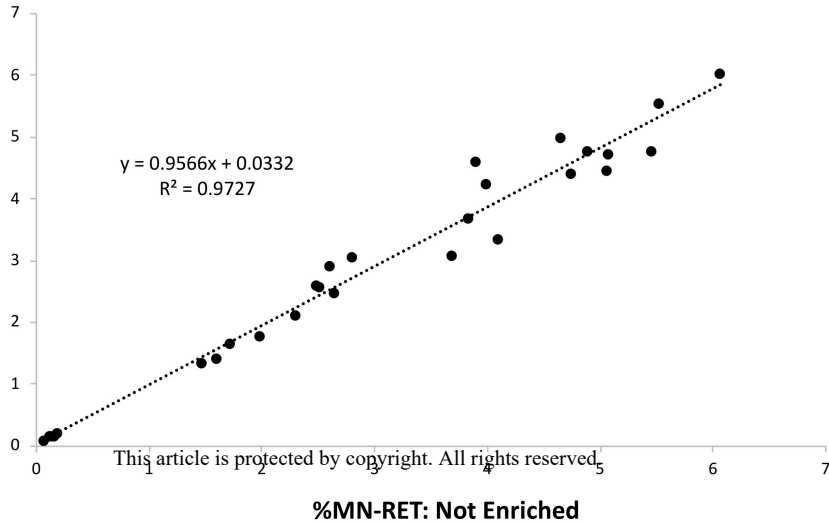
- Horibata, K., Ukai, A., Ishikawa, S., Sugano, A. and Honma, M. (2016) Monitoring genotoxicity in patients receiving chemotherapy for cancer: Application of the *PIG-A* assay. *Mutation Research*, 808, 20-26.
- Khattab, M., Walker, D.M., Albertini, R.J., Nicklas, J.A., Lunblad, L.K.A., Vacek, P.M. and Walker, V.E. (2017) Frequencies of micronucleated reticulocytes, a dosimeter of DNA double-strand breaks, in infants receiving computed tomography or cardiac catheterization. *Mutation Research*, 820, 8-18.
- MacGregor, J., Wehr, C, and Gould, G. (1980) Clastogen-induced micronuclei in peripheral blood erythrocytes: the basis of an improved micronucleus test. *Environmental Mutagenesis*, 2:509-514.
- MacGregor, J.T., Wehr, C.M., Hiatt, R.A., Peters, B., Tucker, J.D., Langlois, R.G., Jacob, R.A., Jensen, R.H., Yager, J.W., Shigenaga, M.K., Frei, B., Eynon, B.P. and Ames, B.N. (1997) 'Spontaneous' genetic damage in man: evaluation of interindividual variability, relationship among markers of damage, and influence of nutritional status. *Mutation Research*, 377, 125-135.
- Offer, T., Ho, E., Traber, M.G., Bruno, R.S., Kuypers, F.A. and Ames, B.N. (2005) A simple assay for frequency of chromosome breaks and loss (micronuclei) by flow cytometry of human reticulocytes. *The FASEB Journal*, 19, 485-487.
- Tometsko, A.M, Torous, D.K. and Dertinger, S.D. (1994) Analysis of micronucleated cells by flow cytometry. 1. Achieving high resolution with a malaria model. *Mutation Research*, 292(2), 129-135.
- Ware, R.E., Rosse, W.F. and Hall, S.E. (1995) Immunophenotypic analysis of reticulocytes in paroxysmal nocturnal hemoglobinuria. *Blood*, 86(4), 1586-1589.
- Witt, K.L., Cunningham, C.K., Patterson, K.B., Kissling, G.E., Dertinger, S.D., Livingston, E., Bishop, J.B. (2007) Elevated frequencies of micronucleated erythrocytes in infants

exposed to zidovudine in utero and postpartum to prevent mother-to-child transmission of HIV. *Environmental and Molecular Mutagenesis*, 48(3-4), 322-329.

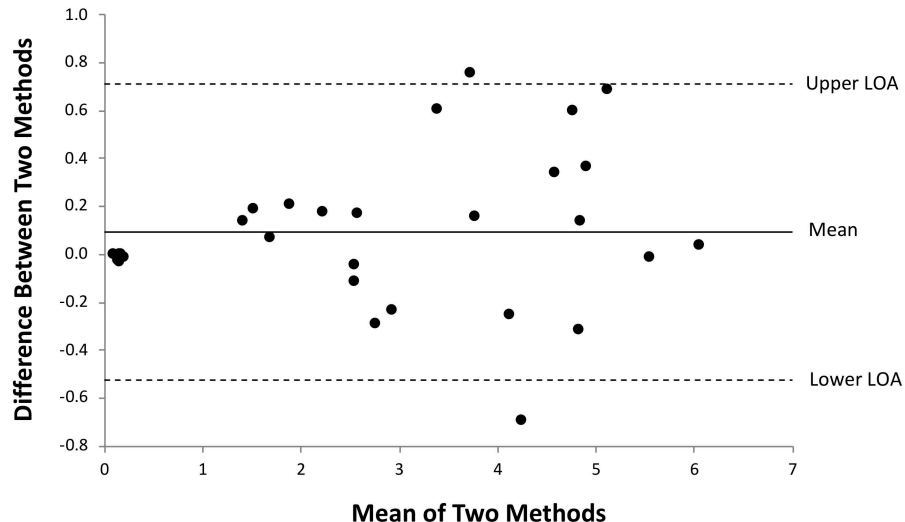
Table I. Subject Information.

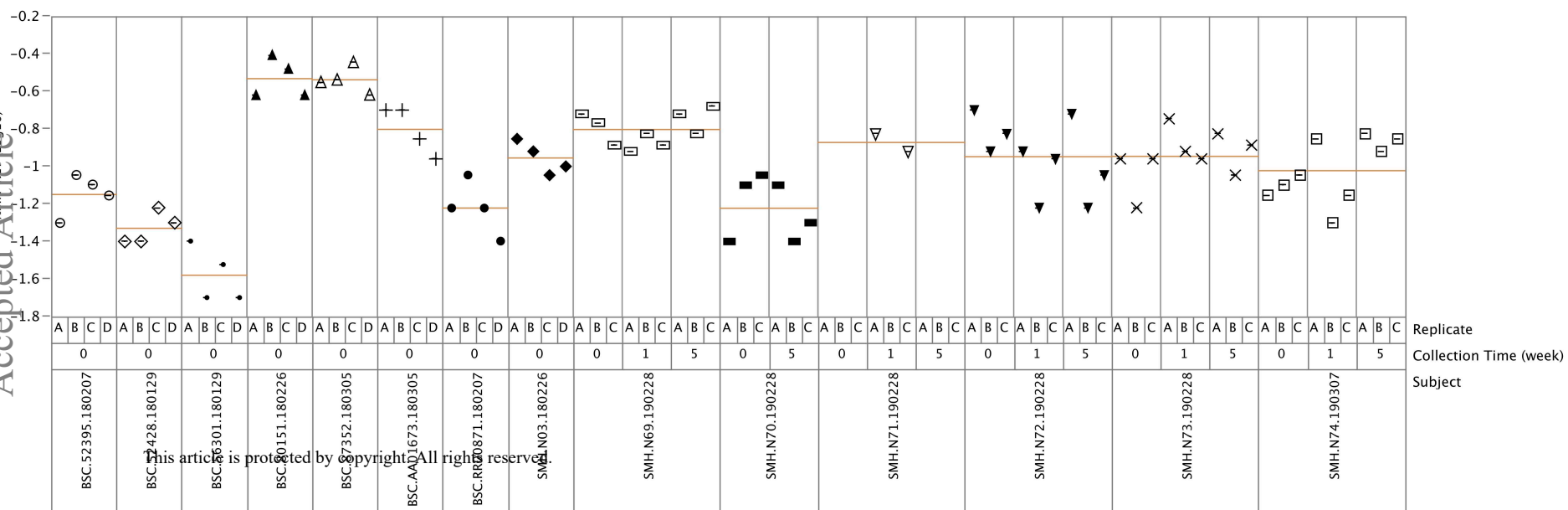
Source	Total No. Subjects (Males/Females)	Age: Range (yr)	Age: Mean \pm Std. Dev. (yr)	Medical Condition
Commercial supplier (Biological Specialty Company)	300 (150/150)	19 - 73	38.2 \pm 12.1	Self-reported healthy adults
URMC, Dept. Radiation Oncology	7 (2/5)	24 - 57	42.1 \pm 11.2	Self-reported healthy adults
Texas Children's Hospital, Dept. Pediatrics	26 (10/16)	0 (cord blood) - 1.2	0.2 \pm 0.3	Healthy (cord bloods) or infants with congenital heart defect
URMC, Dept. Pediatrics	30 (11/19)	8 - 17	14.3 \pm 3.0	Constipation or irritable bowel syndrome; otherwise healthy

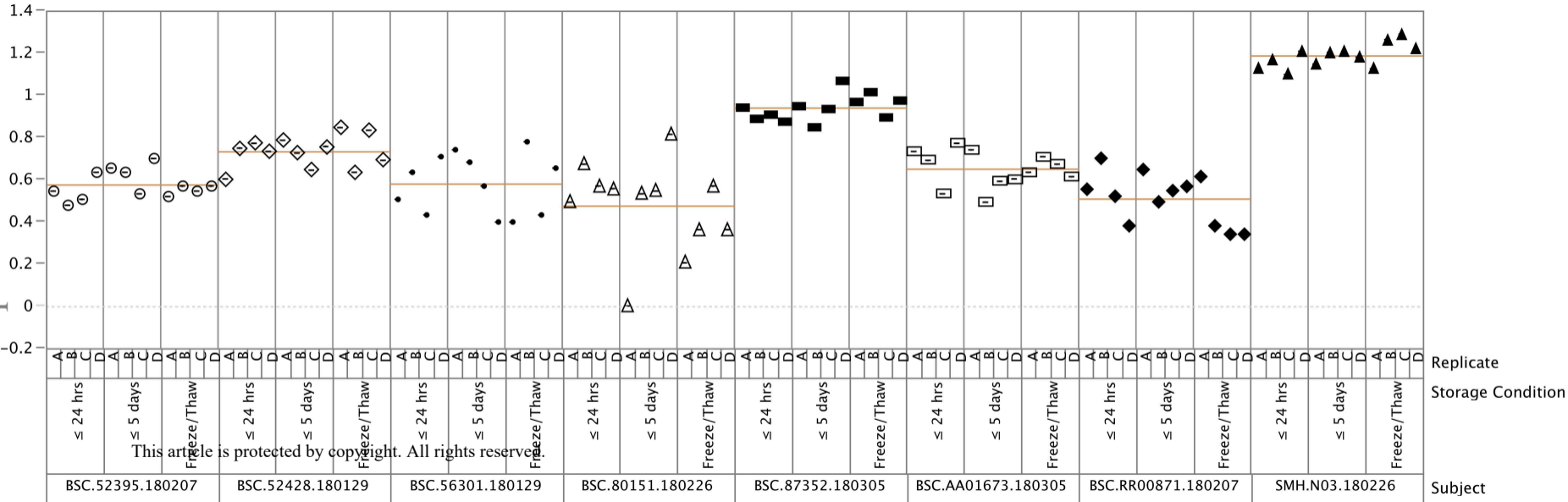
%MN-RET: With vs. Without Enrichment

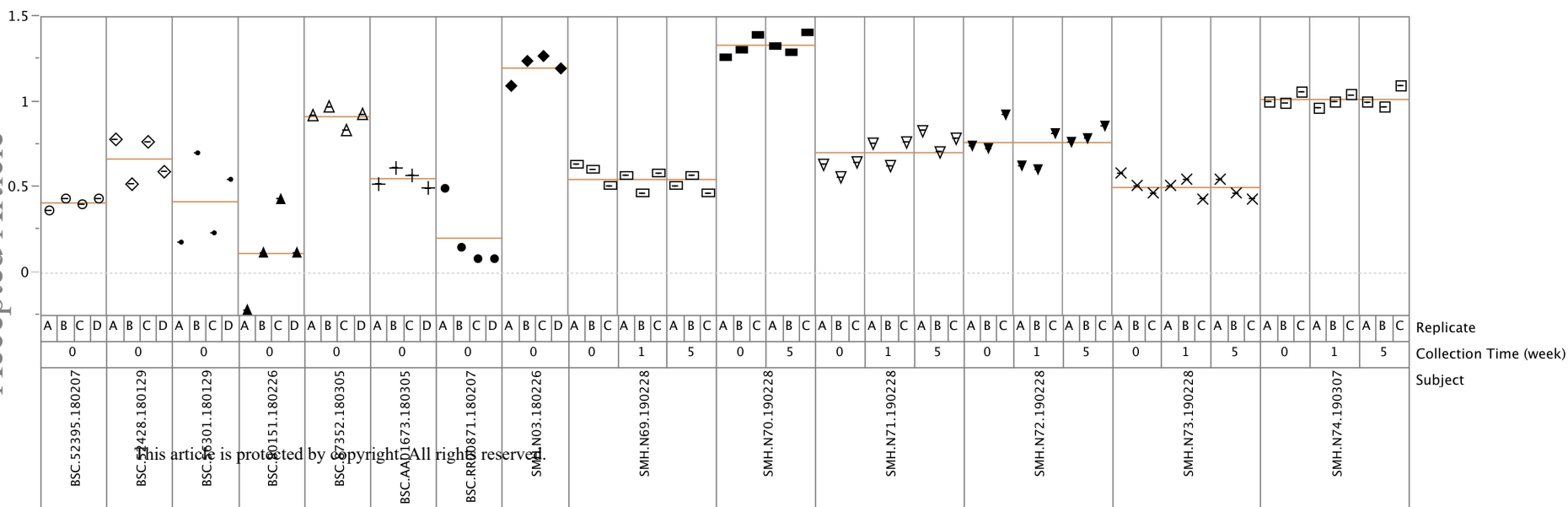


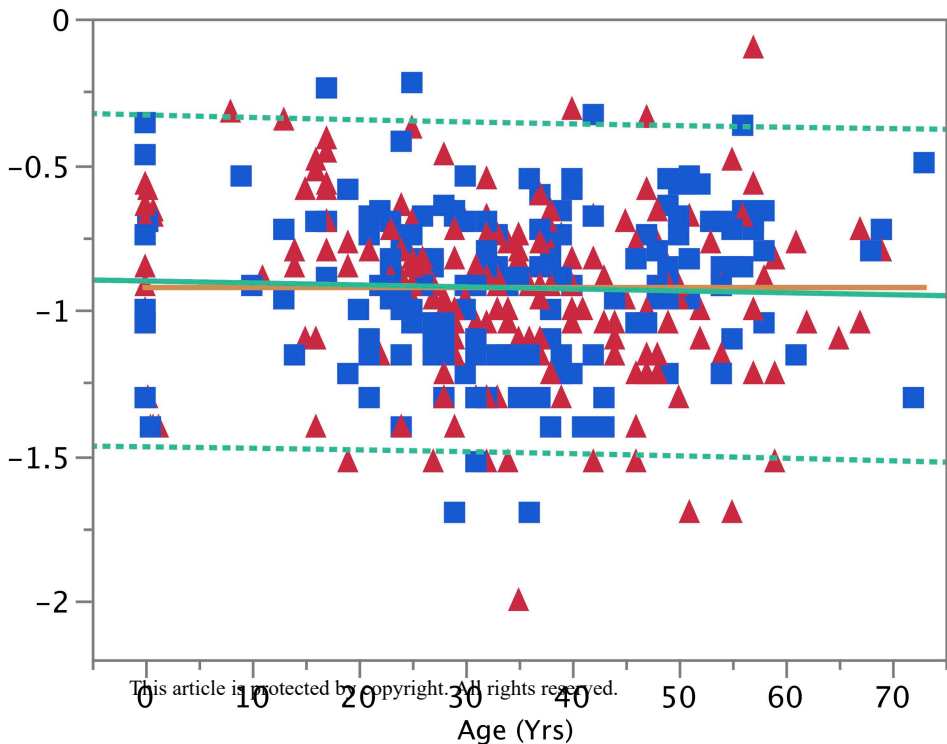
%MN-RET: Bland-Altman Plot



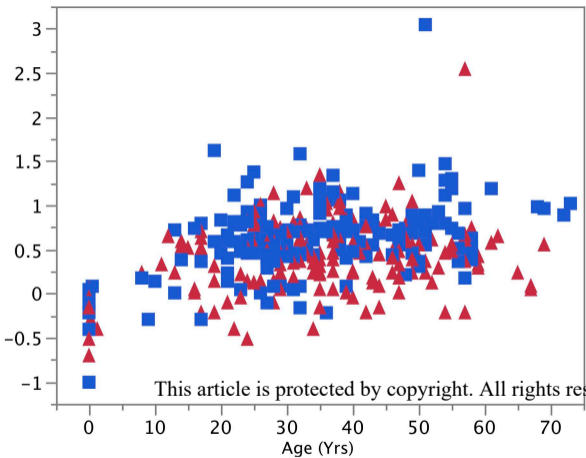




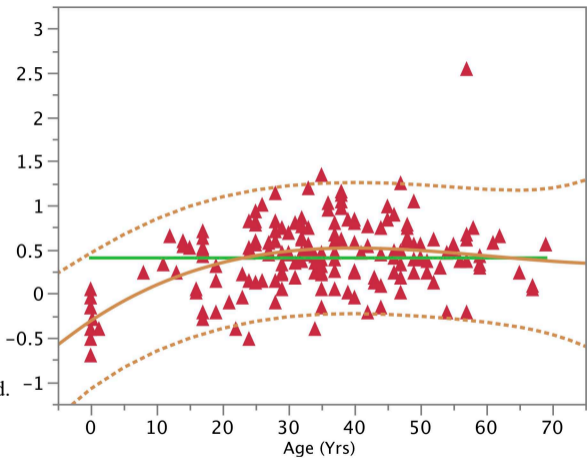




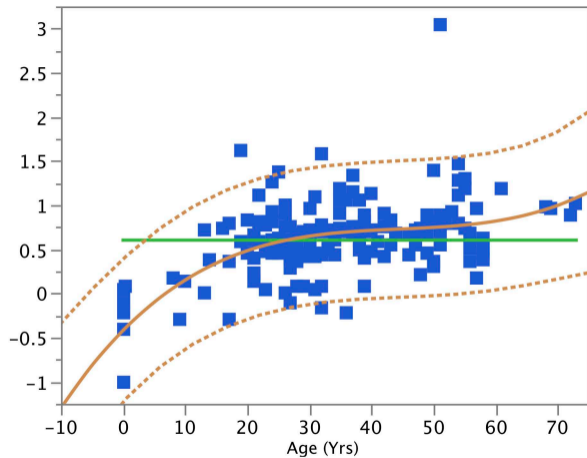
No. Mutant RET per Million (Log10)

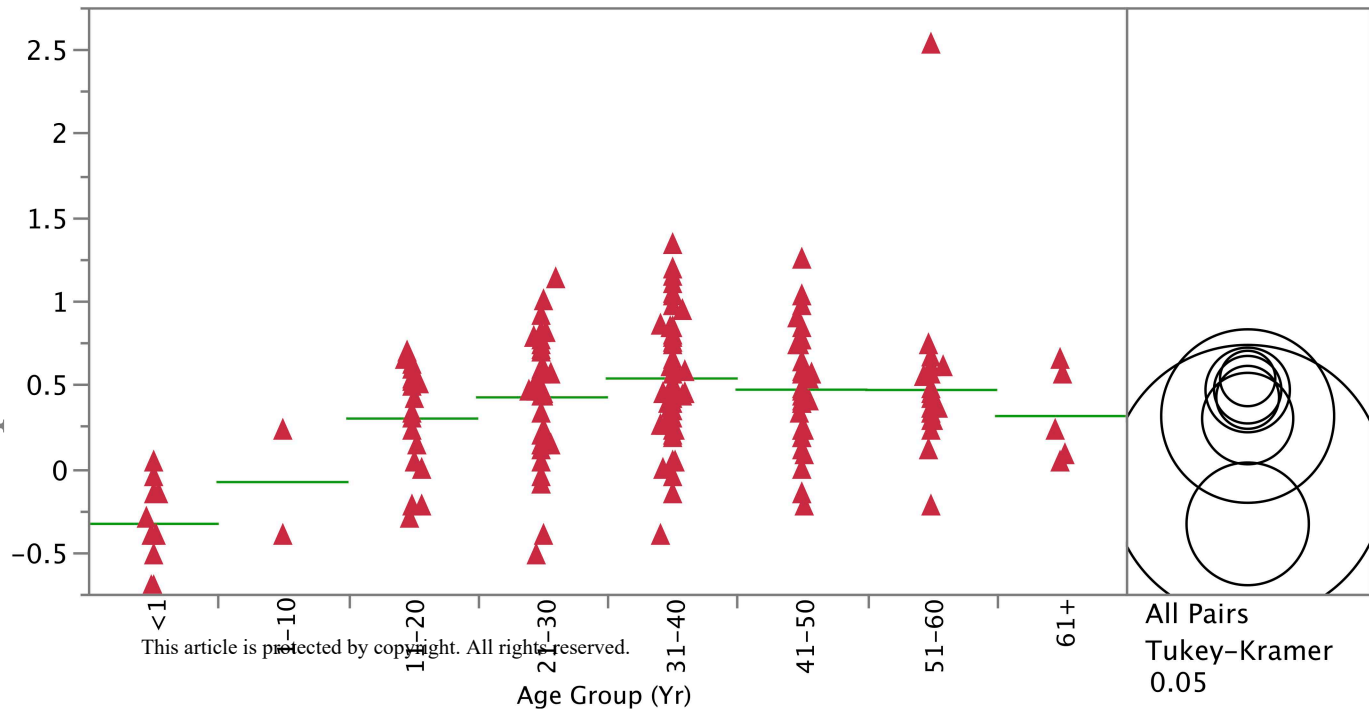


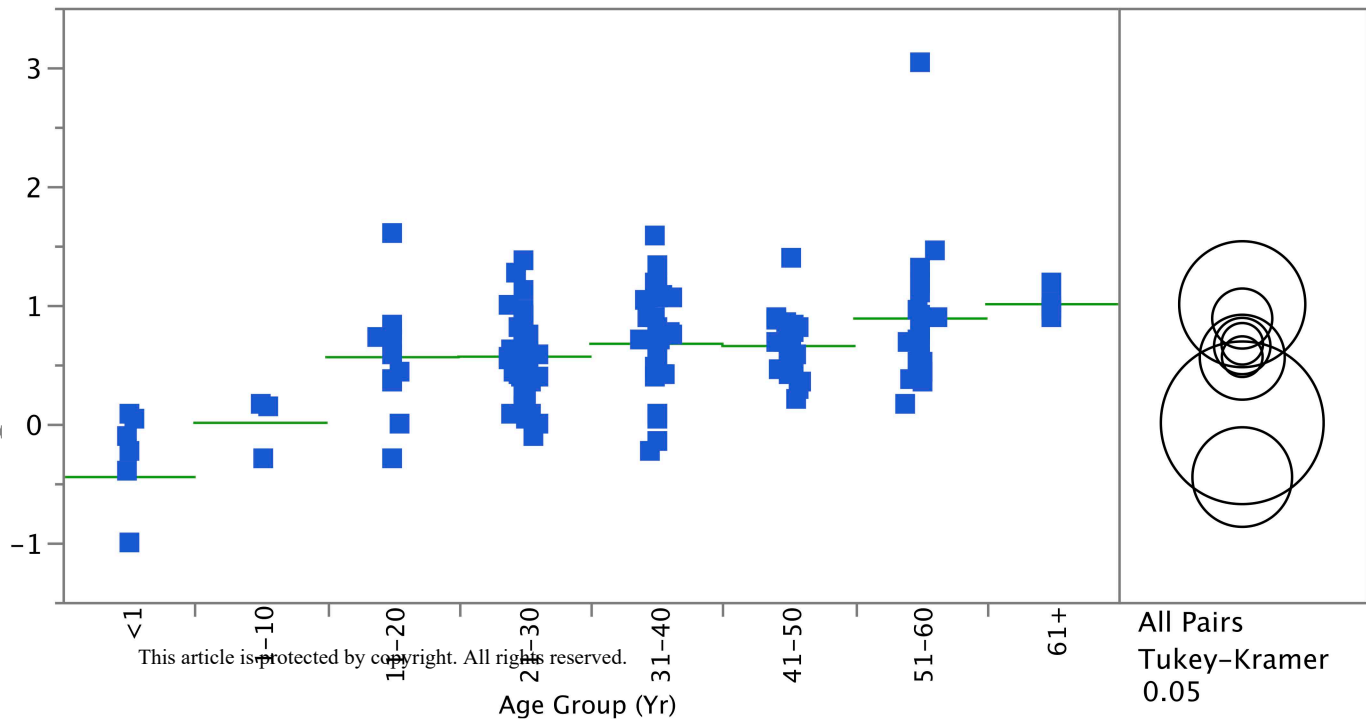
No. Mutant RET per Million (Log10)

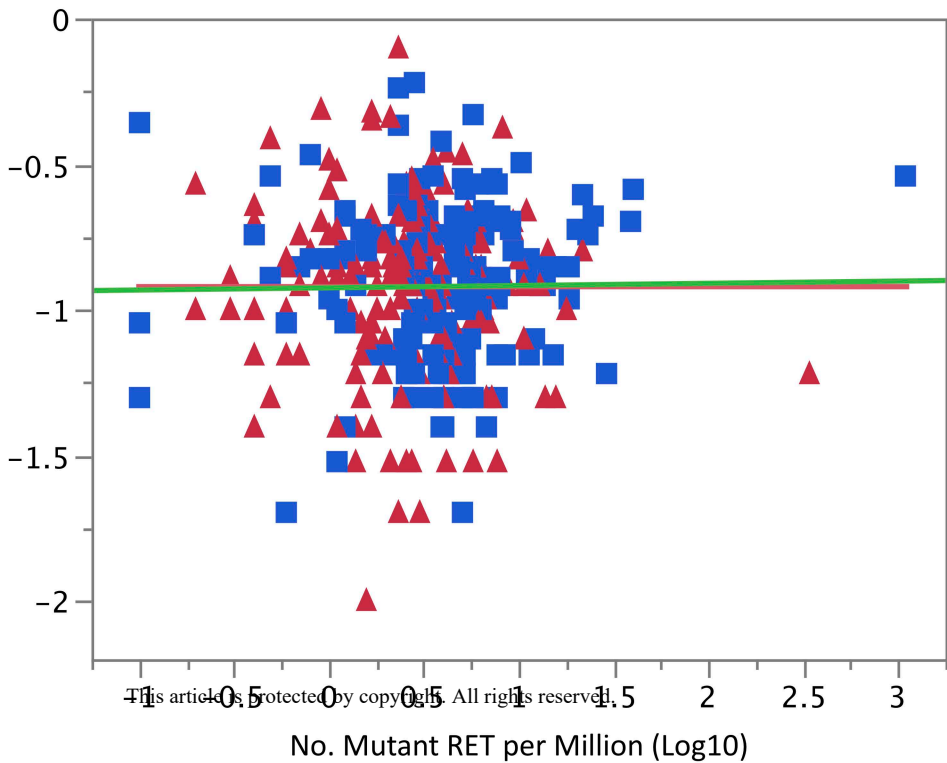


No. Mutant RET per Million (Log10)

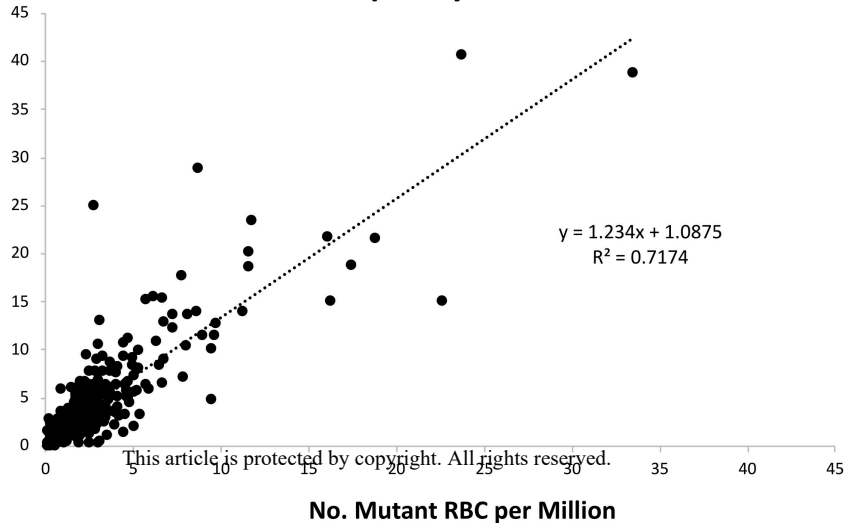








Mutant Cell Frequency: RET vs RBC Cohort



Bland-Altman: RET vs. RBC Cohort

